

# Process of pyroplastic shaping for special-purpose porcelain stoneware tiles

Mariarosa Raimondo<sup>a</sup>, Chiara Zanelli<sup>a</sup>, Guia Guarini<sup>a</sup>, Michele Dondi<sup>a,\*</sup>,  
Roberto Fabbroni<sup>b</sup>, Tiziano Cortesi<sup>b</sup>

<sup>a</sup> *Istituto di Scienza e Tecnologia dei Materiali Ceramici, CNR-ISTEC, 48018 Faenza, Italy*

<sup>b</sup> *Keser Diva Design S.p.A., via San Silvestro 1, 48018 Faenza, Italy*

Received 31 March 2008; received in revised form 7 October 2008; accepted 24 October 2008

Available online 17 November 2008

## Abstract

A novel technique to manufacture special-purpose tiles (i.e. trim pieces, steps, skirting boards, etc.) has been recently developed on the basis of a pyroplastic shaping of porcelain stoneware tiles. This innovative process involves a second firing, peaking at temperatures close to those of sintering, whose effect was investigated by comparing industrially manufactured tiles before and after pyroplastic shaping. Characterization by XRF, XRPD, SEM and standard testing (ISO 10545) put in evidence that pyroplastic bending induced little changes in the water absorption and bulk density values, as in phase composition. Limited variations occurring to closed porosity, mechanical strength and microstructure do not significantly affect the overall technological performance of the special-purpose tiles, which is substantially the same of the original porcelain stoneware tiles. A detailed microstructural characterization was performed for the first time on porcelain stoneware tiles: coarse grains (>10 µm) represent 10–15% of total volume, while fine-grained crystals, dispersed in the glassy phase, amount from 30% to 65% of the viscous matrix. The pyroplastic behaviour was found to depend in a complex way on such microstructural and compositional features, which deeply affect the effective viscosity of the matrix.

© 2008 Elsevier Ltd and Techna Group S.r.l. All rights reserved.

**Keywords:** Ceramic tiles; Porcelain stoneware; Pyroplastic deformation; Trim pieces

## 1. Introduction

Porcelain stoneware tiles are characterized by very low values of water absorption (<0.5% according to the ISO 13006 standard [1]) and usually by 93–97% of theoretical density [2,3]. Such densification is achieved by reactive viscous flow sintering involving the formation, at temperatures over 1100 °C, of a large amount of liquid phase (50–70 wt.%) by melting feldspars and partially quartz and clay minerals [4–6]. Geometrical features of porcelain stoneware tiles are maintained managing fast firing schedules (typically 60 min cold-to-cold with 5–10 min soaking at temperatures ranging from 1190 to 1230 °C) in roller kilns [7]. Even though the temperature control is accurate within 5 °C, the fast kinetics of viscous phase formation and flow makes it easy the appearance of

incipient pyroplastic deformations (e.g. tile expansion and warping) [8–10].

The high temperature behaviour of porcelain stoneware tiles has been exploited to develop an innovative technique able to produce special-purpose tiles (i.e. trim pieces, steps, bullnose, skirting boards, handrails, etc.) [11]. This kind of tiles are conventionally manufactured by isostatic pressing or slip casting and a great effort is required to accurately reproduce the aesthetic design and coloration of the porcelain stoneware tiles, which the special-purpose tiles are combined in floorings and wall coverings [12]. The new technique – which is currently applied in an industrial plant in Italy – is based on pyroplastic shaping of porcelain stoneware tiles, with the great advantage to by-pass the laborious stage of reproducing their aesthetic appearance. It consists of a second firing at a temperature below that of sintering (e.g. 1160–1210 °C) but with a longer firing time and slower thermal rates (e.g. 160–270 min cold-to-cold) in order to avoid heating and/or cooling ruptures [13]. Pyroplastic deformation is overguided by means of refractory supports and some thin grooves ground in the back of the porcelain stoneware tile (Fig. 1).

\* Corresponding author at: Istituto di Scienza e Tecnologia dei Materiali Ceramici, CNR-ISTEC, Consiglio Nazionale delle Ricerche, Via Granarolo 64, 48018 Faenza, Italy. Tel.: +39 0546 699728; fax: +39 0546 46381.

E-mail address: [michele.dondi@istec.cnr.it](mailto:michele.dondi@istec.cnr.it) (M. Dondi).

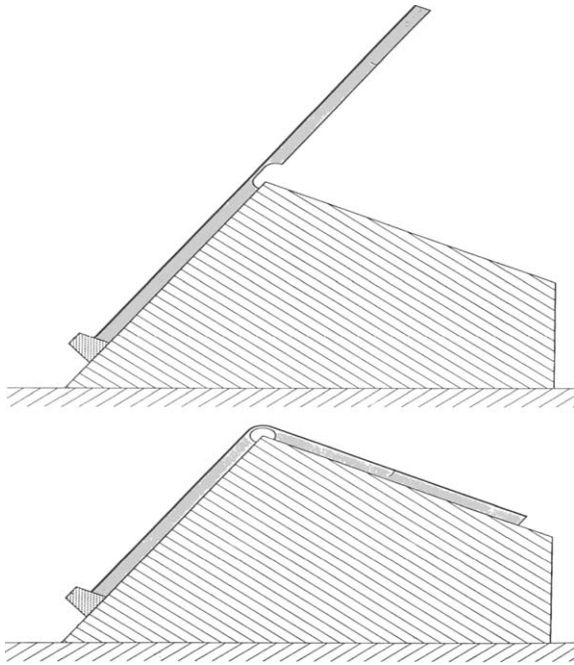


Fig. 1. Pyroplastic shaping process to get special-purpose tiles starting from porcelain stoneware tiles [11].

Pyroplastic deformation implies the occurrence of local rearrangements with possible microstructural changes, perhaps involving development of closed porosity, which might affect the mechanical strength and other technological properties of porcelain stoneware tiles [8–10,14,15]. The aim of the present study is to assess the effect of pyroplastic shaping on the technological performance, microstructure and phase composition by comparing industrially manufactured porcelain stoneware tiles with the correspondent special-purpose tiles.

## 2. Experimental

Nine commercial porcelain stoneware tiles were selected from four different tile manufacturers in order to get a wide range of body composition, tile thickness, technological properties and firing behaviours (Tables 1 and 2). These tiles underwent the industrial pyroplastic shaping process to achieve the correspondent special-purpose tiles, each by its own

Table 1  
Porcelain stoneware tiles selected and temperature of the industrial process of pyroplastic deformation to get special-purpose tiles.

Sample	Porcelain stoneware type	Tile thickness (mm)	Temperature of industrial pyroplastic shaping (°C)
CE	Glazed	8.8	1210
CO	Unglazed	7.5	1180
IN	Unglazed	7.1	1180
KD	Glazed	9.6	1175
KO	Glazed	10.5	1175
KT	Glazed	10.8	1195
LI	Glazed	8.2	1210
OS	Glazed	9.2	1160
RU	Glazed	12.0	1160

Table 2

Chemical composition (wt.%) of porcelain stoneware bodies.

	CE	CO	IN	KD	KO	KT	LI	OS	RU
SiO <sub>2</sub>	73.70	73.96	74.31	72.96	69.47	69.75	74.71	69.79	69.36
TiO <sub>2</sub>	0.43	0.45	0.42	0.33	0.46	0.55	0.67	0.56	0.72
ZrO <sub>2</sub>	1.52	0.14	0.15	1.61	2.93	3.11	0.14	0.19	0.24
Al <sub>2</sub> O <sub>3</sub>	16.25	16.23	15.84	16.42	18.04	17.88	16.13	19.21	19.35
Fe <sub>2</sub> O <sub>3</sub>	0.73	0.79	0.72	0.90	1.11	0.52	0.77	0.66	0.63
MgO	0.44	0.45	0.50	0.42	0.30	0.40	0.50	0.72	0.75
CaO	1.62	1.56	1.60	1.38	1.27	1.29	1.64	1.89	1.93
Na <sub>2</sub> O	2.95	4.02	4.04	4.42	4.88	4.93	3.07	5.36	5.55
K <sub>2</sub> O	2.37	2.40	2.42	1.55	1.55	1.57	2.38	1.62	1.47

appropriate firing schedule, which was set up on the basis of empirical trials carried out in the industrial furnace (Table 1).

Porcelain stoneware tiles were characterized by determining:

- Chemical composition by wavelength-dispersive X-ray fluorescence spectrometry (XRF-WDS, P1480, Philips, Almelo, The Netherlands) on glassy disk obtained by alkaline fusion (Fluxy, Claisse, Sainte-Foy, Canada).
- Pyroplastic deformation was measured as the maximum displacement occurring at the specimen centre ( $\delta_{\max}$ ) after firing in laboratory electric kiln (20 °C/min, 1180 °C maximum temperature, 5 min soaking); five bars, cut from each industrial tile sample (25 cm length  $\times$  2 cm width  $\times$  tile thickness) were put in the kiln on two refractory pins at a span length of 20 cm. A creep rate was calculated on the basis of deflection data and soaking time.
- Uniaxial viscosity ( $E_p$ ) was calculated according to Lee et al. [16]:

$$E_p = \frac{5\rho g L^2}{32\delta_{\max} h^2}$$

where  $\rho$  is the bulk density of the body,  $g$  is the gravitational constant,  $L$  is the span length,  $\delta_{\max}$  is the pyroplastic deformation and  $h$  is the tile thickness.

- Chemical composition of the vitreous phase was calculated on the basis of bulk chemistry and phase composition; it allowed the estimation of the kinematic viscosity of liquid phase into porcelain stoneware bodies [17,18].

Both porcelain stoneware and special-purpose tiles were characterized by determining:

- Phase composition by X-ray powder diffraction (XRPD, D-500, Siemens, Berlin, Germany) and the Rietveld-RIR method using the GSAS-EXPGUI software [19,20] adding 10 wt.% alumina as reference material, to get quantitative results [21]; the amount of glassy phase was calculated by difference to 100% of the sum of crystalline phases.
- Microstructure was investigated by scanning electron microscopy (SEM, Stereoscan 360, Leica, Cambridge, UK) on gold-sputtered polished or etched surfaces (20% HF for 10 s); four photomicrographs for each sample underwent image analysis (Image Pro Plus 4) determining the amount, size and shape of grains coarser than 10  $\mu\text{m}$ . In

Table 3  
Pyroplastic deformation of porcelain stoneware tiles (1180 °C, 5 min soaking).

Sample	Creep rate $\dot{\epsilon}_{\text{exp}}$ ( $\times 10^{-4} \text{ s}^{-1}$ )		Uniaxial viscosity, $E_p$ (GPa s)	
	Mean	S.D.	Mean	S.D.
CE	1.81	0.24	2.00	0.21
CO	4.63	0.52	1.12	0.12
IN	5.36	0.05	1.01	0.11
KD	2.29	0.25	1.38	0.15
KO	4.47	0.13	0.67	0.07
KT	1.50	0.19	1.80	0.19
LI	2.78	0.35	1.51	0.16
OS	1.61	0.19	1.79	0.19
RU	2.00	0.33	0.93	0.10

particular, the amount was quantified as grain volume (polygonal area of the object's outline); particle size as the diameter passing through object centroid; particle shape as the aspect ratio between major and minor axes of the ellipse equivalent to the object.

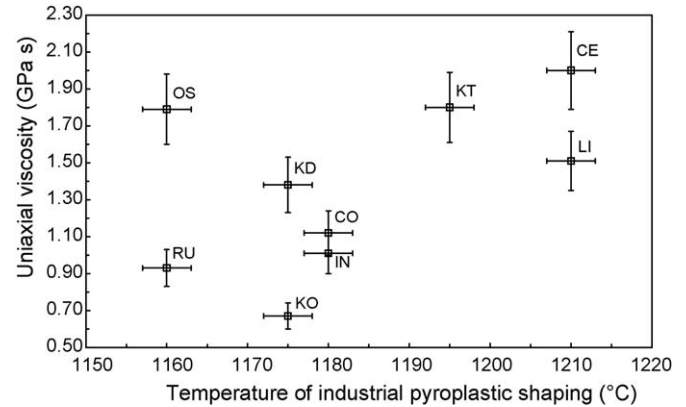


Fig. 2. Temperature of industrial pyroplastic shaping versus uniaxial viscosity of porcelain stoneware tiles.

- (g) Water absorption, open porosity ( $P_o$ ) and bulk density ( $D_b$ ) according to the ISO 10545-3 standard [22].  
(h) Real density ( $D_r$ ) by Helium pycnometry (MPV 1305, Micromeritics, Norcross, USA).

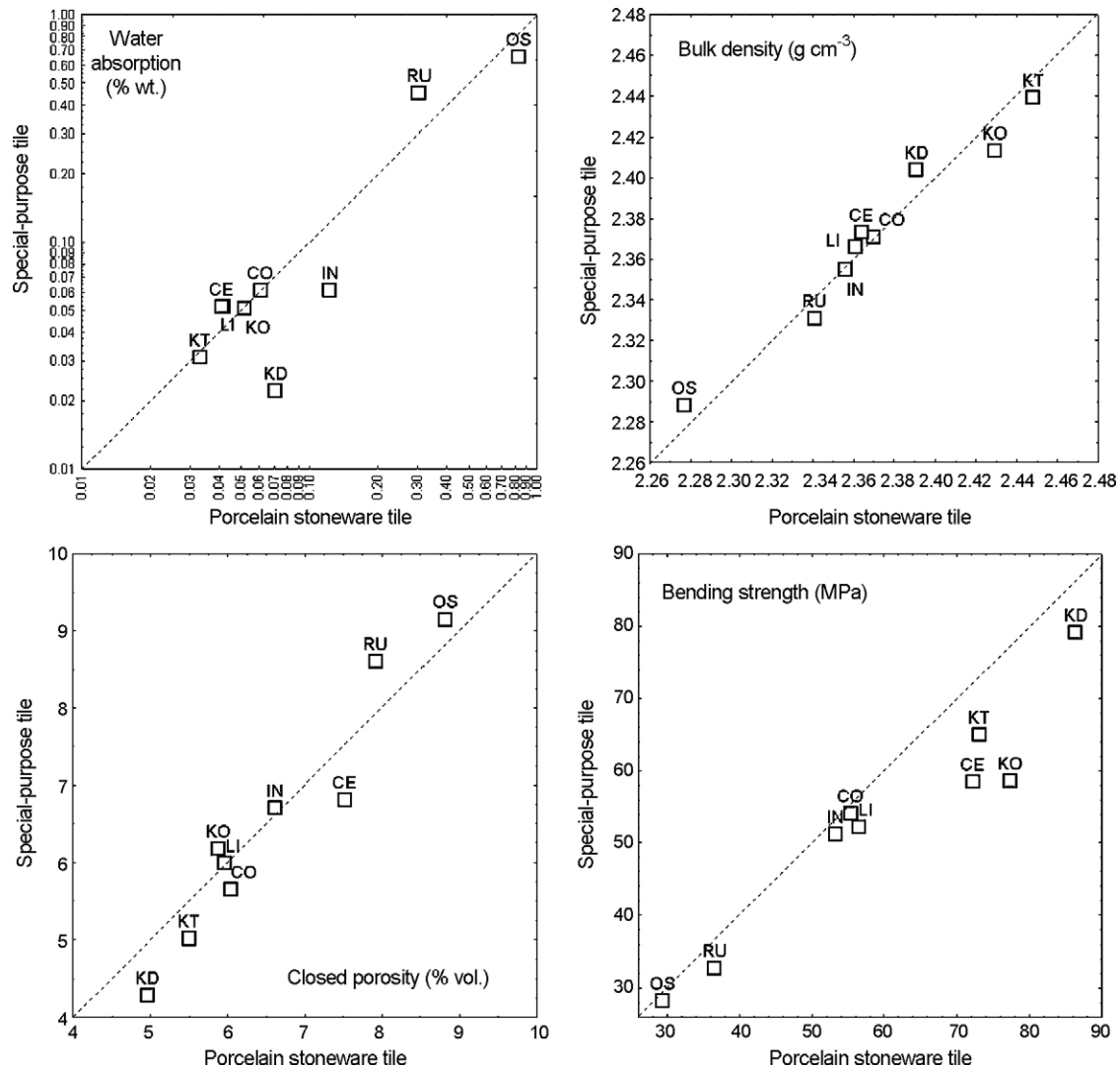


Fig. 3. Effect of the pyroplastic deformation process on technological performance: comparison of the as-received porcelain stoneware tiles with the correspondent special-purpose tiles.

Table 4

Technological properties (mean  $\pm$  standard deviation) of porcelain stoneware tiles. Pyroplastically shaped, special-purpose tiles are indicated by asterisk.

Sample	Water absorption (wt.%)	Porosity (vol.%)			Bulk density $D_b$ (g cm <sup>-3</sup> )	Bending strength (MPa)
		Open ( $P_o$ )	Closed ( $P_c$ )	Total ( $P_t$ )		
CE	0.04 $\pm$ 0.01	0.09 $\pm$ 0.02	7.51 $\pm$ 0.38	7.60 $\pm$ 0.38	2.364 $\pm$ 0.003	72.2 $\pm$ 3.7
CE*	0.05 $\pm$ 0.02	0.13 $\pm$ 0.05	6.80 $\pm$ 0.34	6.93 $\pm$ 0.35	2.373 $\pm$ 0.002	58.4 $\pm$ 4.2
CO	0.06 $\pm$ 0.01	0.15 $\pm$ 0.03	6.04 $\pm$ 0.30	6.19 $\pm$ 0.31	2.370 $\pm$ 0.009	55.4 $\pm$ 3.2
CO*	0.06 $\pm$ 0.01	0.14 $\pm$ 0.03	5.65 $\pm$ 0.28	5.79 $\pm$ 0.29	2.371 $\pm$ 0.003	54.1 $\pm$ 2.6
IN	0.12 $\pm$ 0.03	0.28 $\pm$ 0.07	6.61 $\pm$ 0.33	6.88 $\pm$ 0.34	2.356 $\pm$ 0.009	53.3 $\pm$ 2.5
IN*	0.06 $\pm$ 0.01	0.14 $\pm$ 0.03	6.70 $\pm$ 0.34	6.84 $\pm$ 0.34	2.355 $\pm$ 0.003	51.2 $\pm$ 2.6
KD	0.07 $\pm$ 0.01	0.17 $\pm$ 0.02	4.96 $\pm$ 0.25	5.14 $\pm$ 0.26	2.391 $\pm$ 0.004	86.4 $\pm$ 7.0
KD*	0.02 $\pm$ 0.02	0.05 $\pm$ 0.04	4.28 $\pm$ 0.21	4.33 $\pm$ 0.22	2.404 $\pm$ 0.003	79.2 $\pm$ 3.4
KO	0.05 $\pm$ 0.02	0.12 $\pm$ 0.05	5.88 $\pm$ 0.29	6.00 $\pm$ 0.30	2.429 $\pm$ 0.004	77.4 $\pm$ 3.9
KO*	0.05 $\pm$ 0.01	0.13 $\pm$ 0.02	6.17 $\pm$ 0.31	6.30 $\pm$ 0.31	2.413 $\pm$ 0.006	58.5 $\pm$ 4.8
KT	0.03 $\pm$ 0.03	0.07 $\pm$ 0.06	5.50 $\pm$ 0.27	5.57 $\pm$ 0.28	2.448 $\pm$ 0.002	73.1 $\pm$ 3.9
KT*	0.03 $\pm$ 0.01	0.07 $\pm$ 0.02	5.01 $\pm$ 0.25	5.07 $\pm$ 0.25	2.439 $\pm$ 0.003	65.0 $\pm$ 6.0
LI	0.04 $\pm$ 0.02	0.09 $\pm$ 0.04	5.96 $\pm$ 0.30	6.05 $\pm$ 0.30	2.361 $\pm$ 0.003	56.6 $\pm$ 5.2
LI*	0.05 $\pm$ 0.02	0.12 $\pm$ 0.05	5.98 $\pm$ 0.30	6.10 $\pm$ 0.31	2.366 $\pm$ 0.002	52.1 $\pm$ 3.7
OS	0.83 $\pm$ 0.12	1.89 $\pm$ 0.27	8.81 $\pm$ 0.44	10.70 $\pm$ 0.54	2.277 $\pm$ 0.004	29.3 $\pm$ 1.1
OS*	0.64 $\pm$ 0.07	1.47 $\pm$ 0.15	9.15 $\pm$ 0.46	10.61 $\pm$ 0.53	2.288 $\pm$ 0.002	28.3 $\pm$ 1.5
RU	0.30 $\pm$ 0.04	0.70 $\pm$ 0.10	7.92 $\pm$ 0.40	8.62 $\pm$ 0.43	2.341 $\pm$ 0.003	36.5 $\pm$ 2.0
RU*	0.44 $\pm$ 0.08	1.02 $\pm$ 0.18	8.60 $\pm$ 0.43	9.62 $\pm$ 0.48	2.331 $\pm$ 0.001	32.8 $\pm$ 1.8

(i) Total porosity  $P_t$ , calculated by the equation:  $P_t = [1 - (D_b/D_p)] \times 100$ .

(j) Closed porosity  $P_c$ , calculated as  $P_c = P_t - P_o$ .

(k) Mechanical resistance according to the ISO 10545-4 standard [23].

(l) Impact resistance according to the UNI EDL 248-UNI 9724/10 standard [24].

### 3. Results and discussion

#### 3.1. Pyroplastic behaviour

Porcelain stoneware tiles exhibit a rather wide range of pyroplastic deformation: the deflection arrow, once expressed as point creep rate, goes from 1.5 to  $5.4 \times 10^{-4} \text{ s}^{-1}$ . A more comprehensive parameter, taking into account also bulk density and thickness of specimens, is the uniaxial viscosity, which ranges from 0.67 to 2.00 GPa s (Table 3).

A reasonable correlation between the temperature of industrial pyroplastic shaping, set up through empirical trials in the industrial furnace, and the uniaxial viscosity of porcelain stoneware tiles can be appreciated (Fig. 2). There is only an outlier (sample OS) likely because of its peculiar microstructure and phase composition (see Sections 3.3 and 3.4) which required a longer soaking time in the second firing.

#### 3.2. Technological properties

A comparison of technological performances of the porcelain stoneware tiles versus the correspondent special-purpose tiles is presented in Fig. 3 and Table 4. Little changes occurred in the values of water absorption, porosity and bulk density after the pyroplastic shaping process, besides it involves a second firing peaking at a bending temperature close to the sintering temperature of porcelain stoneware tiles.

More in detail, it can be appreciated from Fig. 3 that both water absorption and bulk density values are slightly affected by pyroplastic bending. Only in two cases the second firing reduced significantly the water absorption (i.e. IN and KD samples). On the other hand, limited variations of closed porosity occurred: denser products (e.g. KD, KT and CO) seem to further reduce their closed porosity after pyroplastic bending, while the OS and RU samples, characterized by relatively high values of total porosity, slightly increase their amount of closed pores.

Mechanical strength is systematically lowered by pyroplastic deformation, even though in a different way for porcelain stoneware tiles with intermediate or low modulus of rupture (i.e. <60 MPa) and for highly resistant porcelain stoneware tiles, whose modulus of rupture is in the 70–90 MPa range. In

Table 5

Impact resistance of porcelain stoneware tiles.

Sample	Bending process		Impact strength (J)	
	Pyroplastically shaped	Groove filled with resin	Tile immersed in sand	Tile not immersed in sand
CO	No	–	n.d.	0.47
	Yes	No	0.62	0.35
	Yes	Yes	0.62	0.59
KD	No	–	n.d.	0.63
	Yes	No	0.66	0.43
	Yes	Yes	0.67	0.63
LI	No	–	n.d.	0.35
	Yes	No	0.62	0.28
	Yes	Yes	0.67	0.51
RU	No	–	n.d.	0.95
	Yes	No	0.49	0.47
	Yes	Yes	0.67	>1.0

n.d. = not determined.



the former, just a limited decrease is observed (on average 5.6%, thus corresponding in many cases to the experimental uncertainty range). In the latter, the drop of modulus of rupture is significant, being from 8% to 24%, but the absolute values are still very high (always >58 MPa) and well over the standard requirement (i.e. >35 MPa) [1].

The impact strength is also affected by pyroplastic bending, being clearly reduced in special-purpose tiles, mainly due to the presence of grooves, which turn to be a potential weakness zone during impact energy dissipation. However, the mechanical performance is fully restored and often improved by filling the grooves with a resin, chosen in order to appropriately fit the elastic and thermal properties of tiles (Table 5).

### 3.3. Microstructure

The microstructure of porcelain stoneware tiles is characterized by a porosity, to a large extent closed, widely variable in amount (up to 10%), size (generally in the 1–50  $\mu\text{m}$  range, but sometimes reaching 100–200  $\mu\text{m}$ ) and shape (rounded

pores commonly dominate, but coalescent or elongated cavities are quite frequent and the pore aspect ratio is on average 1.5) [3,25–27].

Among the samples under investigation, three classes of porcelain stoneware can be distinguished on the basis of porosity (Fig. 4):

- Low porosity stonewares (e.g. KT, total porosity 5.5%, bulk density  $2.45 \text{ g cm}^{-3}$ ) exhibit a very compact texture with predominantly small-sized (mostly <30  $\mu\text{m}$ ) and isodiametrical pores. These kind of products are slightly affected by the second firing, as no changes are discernible in terms of amount, size and shape of pores.
- Intermediate porosity stonewares (e.g. CE, total porosity 7.6%, bulk density  $2.36 \text{ g cm}^{-3}$ ) show a less dense structure, with several pores in the 30–50  $\mu\text{m}$  range. Rounded pores predominate, but irregularly shaped cavities are frequent. Little microstructural changes occur in these materials, consisting in some cases in limited phenomena of pore growth.

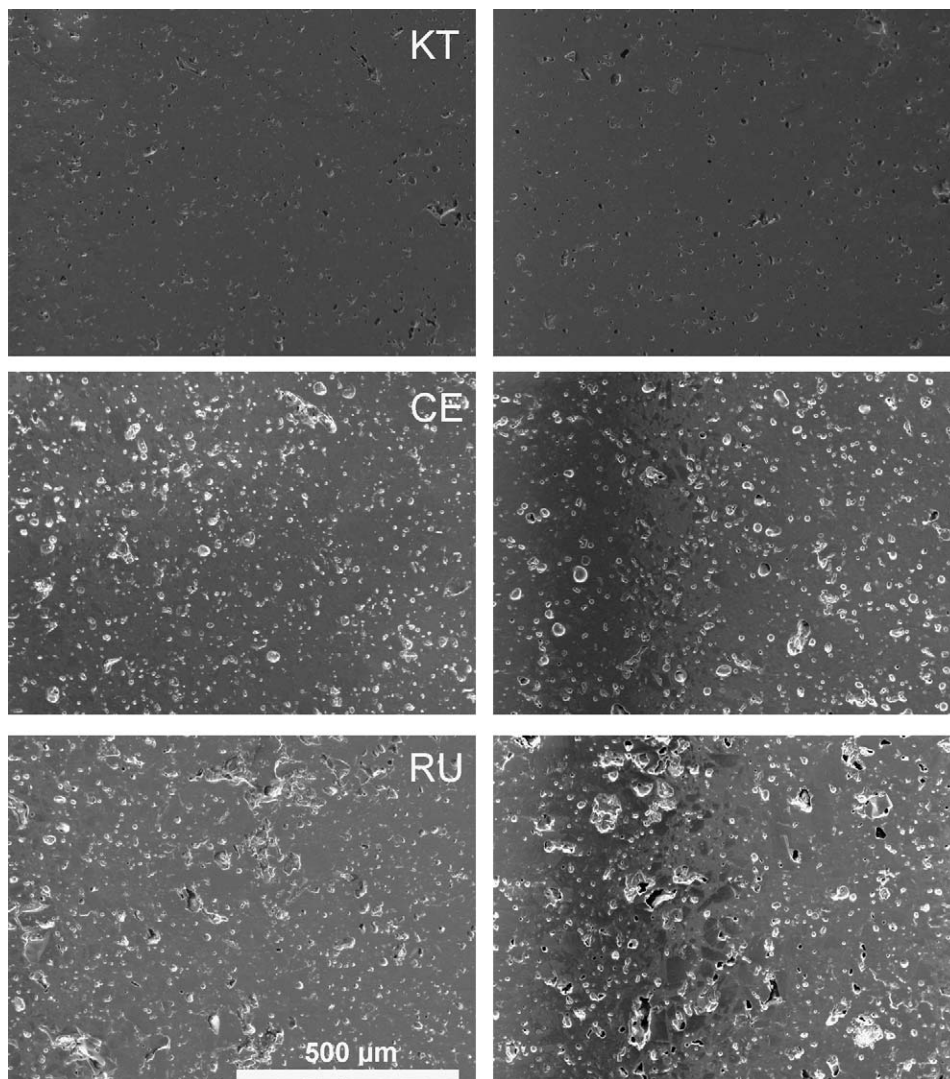


Fig. 4. Microstructure of as-received porcelain stoneware tiles (left) and the correspondent special-purpose tiles (right) under SEM. Samples representative of low porosity (KT), intermediate porosity (CE) and high porosity tiles (RU).

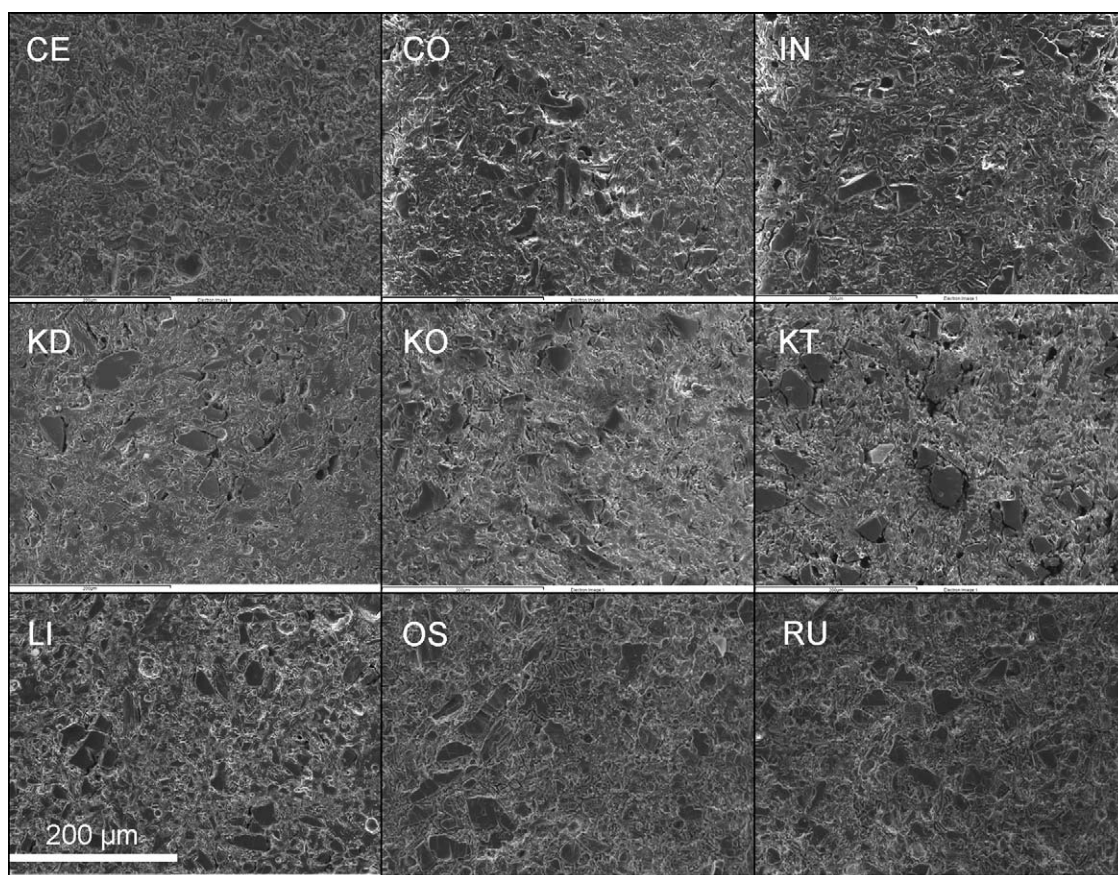


Fig. 5. Microstructure of as-received porcelain stoneware tiles under SEM (etched surface).

- High porosity stonewares (e.g. RU, total porosity 8.6%, bulk density  $2.34 \text{ g cm}^{-3}$ ) represent a special class of tiles characterized by a relatively large amount of coarse (50–200  $\mu\text{m}$ ) and irregularly shaped pores. This type of microstructure undergoes both a pore coarsening, particularly affecting the coarser cavities, and crystal growth.

Since the pyroplastic behaviour of porcelain-like materials is affected by microstructural constraints, the amount, size and shape of coarser grains were determined by image analysis on etched surface (Fig. 5). The average microstructural parameters

are rather similar in all samples: the amount of coarse grains is always in the 11–15% range and the grain diameter is between 18 and 21  $\mu\text{m}$ , with the single exception of sample OS (25  $\mu\text{m}$ ), while the aspect ratio ranges from 1.64 to 1.77 (Table 6). However, both particle size and shape present a large standard deviation, implying a significant non-uniformity of data populations. In effect, particle sizes are widely distributed in the 10–50  $\mu\text{m}$  range, but samples are quite similar each other, but the samples OS and CO which are the coarsest one and the finest one, respectively (Fig. 6A). Also the aspect ratios exhibit some fluctuations with particle size (Fig. 6B).

Table 6  
Microstructural features (amount, size and shape of grains coarser than 10  $\mu\text{m}$ ) of porcelain stoneware tiles.

Sample	Grain volume (%)		Grain aspect ratio (1)		Grain diameter ( $\mu\text{m}$ )	
	Average	S.D.	Average	S.D.	Average	S.D.
CE	13.0	0.2	20.2	8.0	1.69	0.53
CO	13.8	0.1	18.1	7.3	1.72	0.45
IN	12.9	0.2	20.8	8.8	1.77	0.54
KD	14.3	0.1	18.7	9.4	1.73	0.57
KO	12.8	0.2	18.6	8.1	1.74	0.55
KT	14.7	0.1	20.2	9.4	1.73	0.49
LI	14.1	0.1	18.0	7.3	1.72	0.45
OS	12.1	0.2	25.2	9.9	1.64	0.45
RU	11.1	0.2	19.2	6.2	1.68	0.49



Table 7

Calculated chemical and normative composition (wt.%), and estimated kinematic viscosity of the glassy phase (at 1180 °C) of porcelain stoneware bodies.

	CE	CO	IN	KD	KO	KT	LI	OS	RU
SiO <sub>2</sub>	67.94	68.87	67.98	69.74	68.00	68.88	68.70	67.04	65.66
TiO <sub>2</sub>	0.72	0.74	0.72	0.49	0.72	0.86	1.07	1.07	1.33
ZrO <sub>2</sub>	0.63	0.12	0.14	0.59	0.27	0.65	0.12	0.24	0.32
Al <sub>2</sub> O <sub>3</sub>	18.21	16.97	17.61	17.19	18.68	18.31	17.76	18.65	19.86
Fe <sub>2</sub> O <sub>3</sub>	1.22	1.30	1.24	1.33	1.74	0.81	1.23	1.26	1.16
MgO	0.74	0.74	0.86	0.62	0.47	0.62	0.80	1.38	1.39
CaO	2.72	2.56	2.76	2.04	1.99	2.01	2.62	3.62	3.57
Na <sub>2</sub> O	4.92	5.31	5.68	6.31	6.38	6.05	4.64	5.74	5.44
K <sub>2</sub> O	2.90	3.39	3.01	1.69	1.76	1.81	3.07	1.00	1.28
Quartz	20.4	18.3	16.0	20.4	18.8	20.6	23.2	19.6	19.0
Plagioclase	55.0	57.5	61.7	63.4	63.8	61.0	52.2	66.5	63.7
Orthoclase	17.1	20.0	17.8	10.0	10.4	10.7	18.1	5.9	7.6
Corundum	2.0	0.0	0.0	1.3	2.7	2.7	2.0	1.5	3.0
Hyperstene	1.8	1.8	2.1	1.5	1.2	1.5	2.0	3.4	3.5
Hematite	1.2	1.3	1.2	1.3	1.7	0.8	1.2	1.3	1.2
Rutile	0.7	0.7	0.7	0.5	0.7	0.9	1.1	1.1	1.3
Zircon	1.3	0.2	0.3	1.2	0.5	1.3	0.2	0.5	0.6
$\eta$ (kPa s)	4.57	3.58	3.67	3.80	3.60	3.60	4.79	4.86	5.75

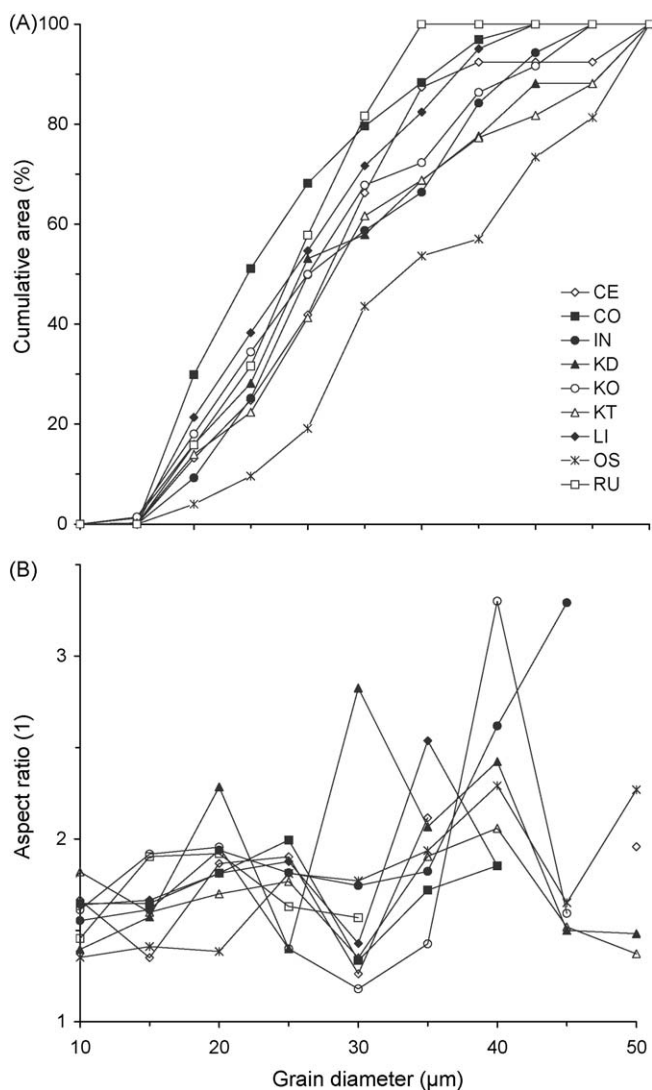


Fig. 6. Particle size distribution (A) and aspect ratio distribution (B) of grains coarser than 10 μm.

### 3.4. Phase composition

The phase composition of porcelain stoneware tiles is characterized by an abundant glassy phase embedding residual quartz, feldspars and zircon as well as new formed mullite and occasionally feldspar [8–10].

Tiles exhibit limited changes after the pyroplastic shaping process (Fig. 7):

- Bodies richer in quartz (i.e. CE, CO, IN, LI) show a diminution in the order of 2%, indicating a limited reactivity of quartz, which partially dissolves in the liquid phase, confirming data on porcelain bodies [8,15,26].
- Coarse-grained bodies (i.e. OS and RU) rich in unreacted feldspars, underwent a considerable crystallization of plagioclase, mostly at expenses of the glassy phase; crystallization phenomena involve to some extent even quartz.
- Changes of K-feldspar, mullite and zircon contents are mostly within the experimental error of the quantitative phase analysis; some crystallization occurred during pyroplastic bending, concerning K-feldspar (CE, LI and RU) and mullite (IN, KO, LI).

The pyroplastic behaviour is affected by the amount and effective viscosity of the liquid phase. The chemical composition of the glassy phase, calculated on the basis of bulk chemistry and phase composition, is illustrated in Table 7, together with the normative composition, i.e. the correspondent fractions of melted minerals. The glassy phase in porcelain stoneware has basically a feldspathic composition (72–80%) with a widely variable Na/K ratio (from 1.5 to 4.3). Along with a remarkable quartz contribution (16–23%), there are small fractions of Mg, Fe, Ti and Zr compounds and a very limited oversaturation in alumina (<3%).

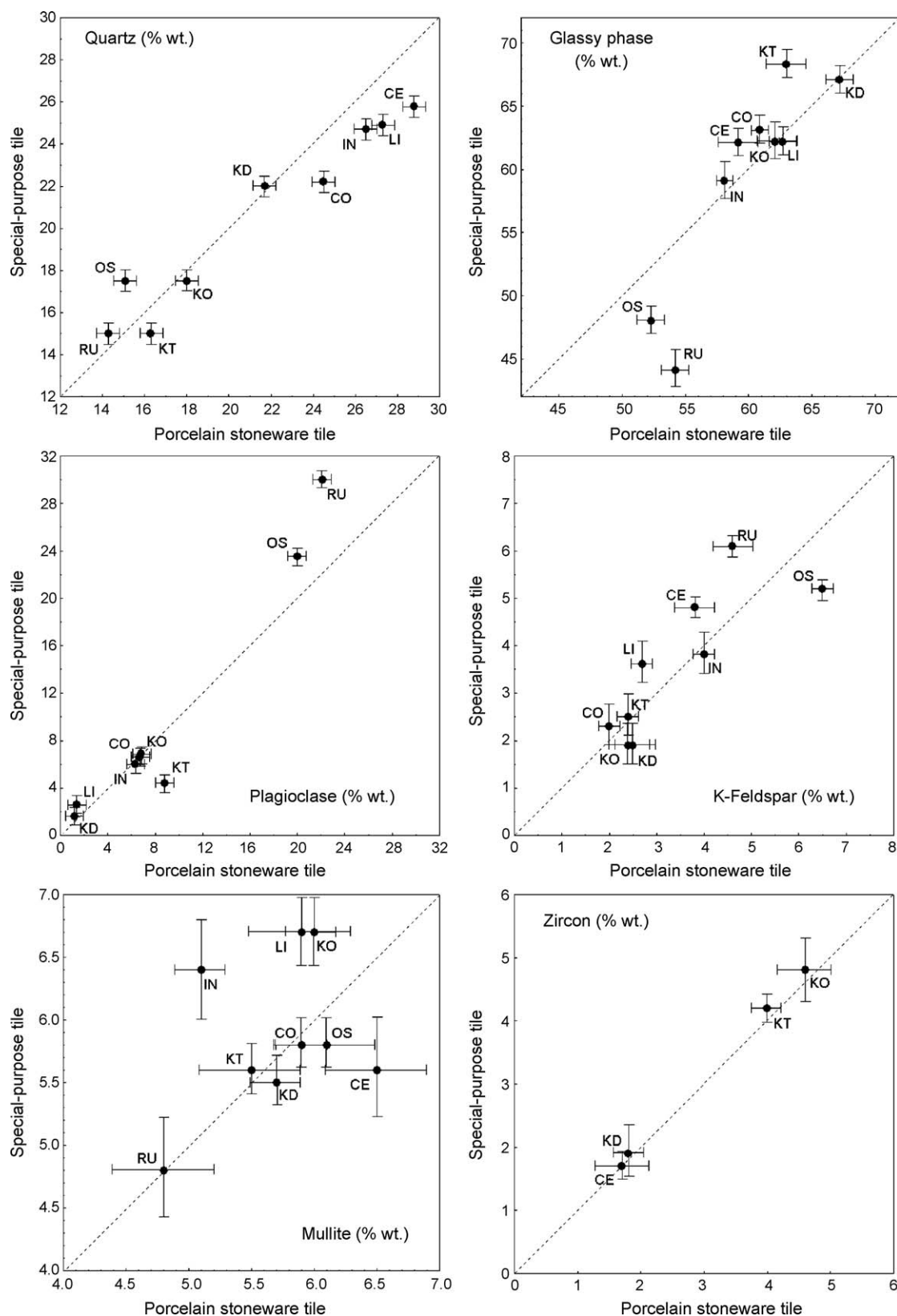


Fig. 7. Effect of the pyroplastic deformation process on phase composition: comparison of the as-received porcelain stoneware tiles with the correspondent special-purpose tiles.



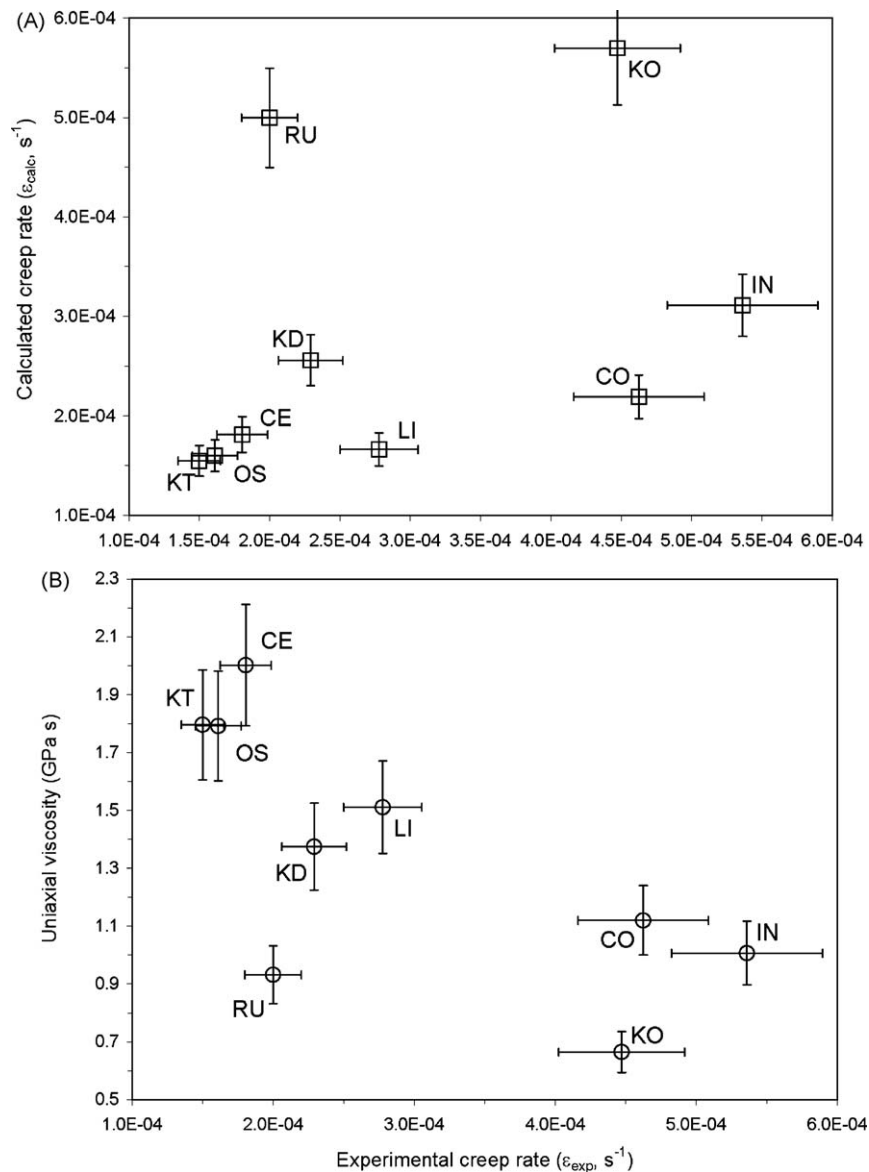


Fig. 8. Pyroplastic behaviour of porcelain stoneware tiles. Experimental creep rate versus (A) calculated creep rate (Eq. (1)) and uniaxial viscosity (B).

These chemical features make the calculated kinematic viscosity of the glassy phase relatively low, being between 3.5 and 6 kPa s at 1180 °C, which is the temperature of pyroplastic testing (Table 7). However, there is no significant correlation between the pyroplastic behaviour and the viscosity of the glassy phase, because account must be taken of small crystalline particles ( $<5 \mu\text{m}$ ) which are dispersed in the liquid phase and contribute to increase dramatically the viscosity of the matrix. Their amount can be estimated by the difference between the total amount of crystalline phases (determined by XRPD) and the amount of grains coarser than  $10 \mu\text{m}$  (determined by image analysis), resulting to be approximately from 20% to 35%. According to this estimation, the viscous matrix of porcelain stoneware (ranging from 84% to 89% of the body) is in reality made up of liquid phase plus 30–65% of fine-grained crystals. This explains the large difference between

viscosity values of glassy phase (in the order of  $10^3 \text{ Pa s}$ ) and the uniaxial viscosity (in the order of  $10^9 \text{ Pa s}$ ).

Even in a simple approach to model the pyroplastic behaviour of porcelain stoneware, there is a strong difficulty to evaluate the viscosity of the matrix (i.e. glassy phase + microcrystals). For instance, in the Dryden's model [28]:

$$\epsilon_{\text{calc}} = \frac{\alpha \sigma (w/d)^3}{\eta} \quad (1)$$

the creep rate ( $\epsilon_{\text{calc}}$ ) depends on the viscosity of the liquid phase ( $\eta$ ), the applied stress ( $\sigma$ ), the grain size ( $d$ ) and the intergranular distance ( $w$ );  $\alpha$  is an adimensional constant. The creep rate, as calculated using data in Tables 3, 6 and 7, does not present any significant correlation once contrasted with the creep rate determined experimentally ( $\epsilon_{\text{exp}}$ ). The result is

improved by using the uniaxial viscosity of the body ( $E_p$ ) instead of the kinematic viscosity of the glassy phase, even if the correlation coefficient is still very low (Fig. 8A). As a matter of fact, uniaxial viscosity is able to explain to a rather large extent the observed pyroplastic behaviour (Fig. 8B). Therefore, the main challenge seems to account for the complex distribution of microstructural parameters, like amount, size and shape of crystalline grains.

#### 4. Conclusions

The innovative technology used to produce special-purpose tiles by pyroplastic bending of porcelain stoneware tiles does not significantly affect the overall technological performance of products, which remains in most cases substantially unchanged.

The second firing, performed to shape the plain porcelain stoneware tiles in steps, skirting boards, trim pieces and so on, has little effect on water absorption, bending strength and phase composition, even if it reaches temperatures close to that of sintering. Different behaviours have been outlined: the denser porcelain stonewares tend to further reduce their own closed porosity, with little repercussions on microstructure, but with a limited loss of mechanical strength, which at any rate remains well over the standard requirement. In contrast, porcelain stonewares with a relatively high closed porosity exhibit some coarsening phenomena, affecting both pores and crystals, but with little effect on mechanical strength.

A detailed microstructural characterization was performed for the first time on porcelain stoneware tiles: coarse grains ( $>10\text{ }\mu\text{m}$ ) represent 10–15% of total volume, while fine-grained crystals, dispersed in the liquid phase, amount from 30% to 65% of the viscous matrix. The pyroplastic behaviour was found to depend in a complex way on such microstructural and compositional features, which deeply affect the effective viscosity of the matrix.

#### Acknowledgement

This work was performed under the financial support of the Regione Emilia-Romagna in the framework of PRRIIT (Programma Regionale per la Ricerca Industriale, l'Innovazione e il Trasferimento Tecnologico, Misura 1, Azione A).

#### References

- [1] ISO 13006, Ceramic Tiles—Definitions, Classification, Characteristics and Marking, International Organization for Standardization, 1998.
- [2] M. Dondi, G. Ercolani, G. Guarini, M. Raimondo, P.M. Cavalcante Tenorio, C. Zanelli, Resistance to deep abrasion of porcelain stoneware tiles: key factors, *Ind. Ceram.* 25 (2) (2005) 71–78.
- [3] M. Dondi, G. Guarini, M. Raimondo, E.R. Almendra, P.M. Cavalcante Tenorio, The role of surface microstructure on the resistance to stains of porcelain stoneware tiles, *J. Eur. Ceram. Soc.* 25 (2005) 357–365.
- [4] M. Dondi, G. Ercolani, M. Marsigli, C. Melandri, C. Mingazzini, The chemical composition of porcelain stoneware tiles and its influence on microstructure and mechanical properties, *InterCeram* 48 (2) (1999) 75–83.
- [5] A.F. Gualtieri, Thermal behavior of the raw materials forming porcelain stoneware mixtures by combined optical and in situ X-ray dilatometry, *J. Am. Ceram. Soc.* 90 (2007) 1222–1231.
- [6] M. Raimondo, C. Zanelli, F. Matteucci, G. Guarini, M. Dondi, J.A. Labrincha, Effect of waste glass (PC/TV screen and cathodic tube) on technological properties and sintering behaviour of porcelain stoneware tiles, *Ceram. Int.* 33 (2007) 615–623.
- [7] A. Salem, S.H. Jazayeri, A. Tucci, G. Timellini, Influence of firing temperature and soaking time on sintering of porcelain stoneware tiles, *CFI-Ceram. Forum Int.* 80 (9) (2003) E66.
- [8] A.M. Buchtel, W.M. Carty, M.D. Noirot, Pyroplastic deformation revisited, *Ceram. Eng. Sci. Proc.* 25 (2) (2004) 24–42.
- [9] A.M. Bernardin, D.S. de Medeiros, H.G. Riella, Pyroplasticity in porcelain tiles, *Mater. Sci. Eng. A* 427 (2006) 316–319.
- [10] E. Rambaldi, W.M. Carty, A. Tucci, L. Esposito, Using waste glass as a partial flux substitution and pyroplastic deformation of a porcelain stoneware tile body, *Ceram. Int.* 33 (2007) 727–733.
- [11] R. Fabbroni, A process for modeling ceramic tiles, Patent WO/2003/080302, applicant Keser Diva Design S.p.A. Faenza.
- [12] G. Guerrieri (Ed.), The end-of-line system and complementary activities, SALA, Modena, 2007, pp. 1–536.
- [13] G. Guerrieri (Ed.), Drying and firing of ceramic tiles, SALA, Modena, 2005, pp. 1–448.
- [14] P.M. Tenorio Cavalcante, M. Dondi, G. Ercolani, G. Guarini, C. Melandri, M. Raimondo, E. Rocha e Almendra, The influence of microstructure on the performance of white porcelain stoneware, *Ceram. Int.* 30 (2004) 953–963.
- [15] W.M. Carty, Glass phase composition in porcelains and correlation with pyroplastic deformation, *Ceram. Eng. Sci. Proc.* 24 (2) (2003) 108–132.
- [16] S.-H. Lee, G.L. Messing, D.J. Green, Bending creep test to measure the viscosity of porous materials during sintering, *J. Am. Ceram. Soc.* 86 (2003) 882–887.
- [17] T. Lakatos, G. Johansson, B. Skimmingskold, Viscosity temperature relations in the glass system  $\text{SiO}_2\text{--Al}_2\text{O}_3\text{--Na}_2\text{O--K}_2\text{O--CaO--MgO}$  in the composition range of technical glasses, *Glass Technol.* 13 (1972) 88–95.
- [18] C. Zanelli, M. Dondi, G. Baldi, G. Ercolani, G. Guarini, M. Raimondo, Glass ceramic frits for porcelain stoneware bodies: effects on sintering, phase composition and technological properties, *Ceram. Int.* 34 (2008) 455–465.
- [19] A.F. Gualtieri, Accuracy of XRPD QPA using the combined Rietveld-RIR method, *J. Appl. Cryst.* 33 (2000) 267–278.
- [20] A.C. Larson, R.B. Von Dreele, Generalized Structure Analysis System, LAUR, Los Alamos, NM, 1999.
- [21] B.H. Toby, EXPGUI, a graphical user interface for GSAS, *J. Appl. Cryst.* 34 (2001) 210–213.
- [22] ISO 10545-3, International Standard for Ceramic tiles—Part 3. Determination of water absorption, apparent porosity, apparent relative density and bulk density, International Organization for Standardization, 1995.
- [23] ISO 10545-4, International Standard for Ceramic tiles—Part 4. Determination of modulus of rupture and breaking strength, International Organization for Standardization, 2000.
- [24] UNI EDL 248-UNI 9724/10, Determination of the impact resistance of building stone (in Italian). UNI, Ente Italiano di Unificazione, 1992.
- [25] G.P. Souza, E. Rambaldi, A. Tucci, L. Esposito, W.E. Lee, Microstructural variation in porcelain stoneware as a function of flux system, *J. Am. Ceram. Soc.* 83 (2004) 1959–1966.
- [26] Y. Iqbal, W.E. Lee, Microstructural evolution in triaxial porcelain, *J. Am. Ceram. Soc.* 83 (2000) 3121–3127.
- [27] Y. Iqbal, W.E. Lee, Fired porcelain microstructures revisited, *J. Am. Ceram. Soc.* 82 (1999) 3584–3590.
- [28] J.R. Dryden, D. Kucerosky, D.S. Wilkinson, D.F. Wyatt, Creep deformation due to a viscous grain boundary phase, *Acta Metall.* 37 (1989) 2007–2015.